Journal of Photopolymer Science and Technology
Volume 15, Number 2 (2002) 231-236 © 2002 TAPJ

Synthesis, Characterization, and Optical Properties of Uniaxially Drawn and Gold Nanoparticle Dispersed Fluorinated Polyimide Films

Satoshi KOIZUMI, Sho-ichi MATSUDA and Shinji ANDO*

Department of Organic & Polymeric Materials, Tokyo Institute of Technology, Ookayama, Meguro-ku, Tokyo, 152-8552, Japan
e-mail : sando@polymer.titech.ac.jp

Gold-nanoparticle dispersed fluorinated polyimide films were prepared by thermal curing and uniaxially drawing of poly(amic acid) films containing hydrogen tetrachloroaurate(III) trihydrate ($HAuCl_4 \cdot 3H_2O$) as a dopant. The chemical states, crystallinity, average sizes, and spatial distribution of the gold particles were examined, and the optical and thermal properties of the films were compared with those of the host-polyimide. The gold salt was converted into zero-valent gold particles having high crystallinity after thermal imidization. TEM micrograph showed that the precipitated gold nanoparticles inside the films are larger than those in the surface area, and they have well-defined lozenge or rectangular shapes, which suggest pressed octahedron or rectangular parallelepiped structures of the crystallites. In addition, their long axes are oriented along the drawing direction and the surface direction. The films show much higher absorption in the visible region than the host-polyimide, which is due to the surface plasmon absorption of gold nanoparticles. In addition, significant anisotropy in optical transmittance are observed for the Au-dispersed films. This supports the orientation of precipitated gold nanoparticles having anisotropic shapes along the drawing direction.
Keywords : gold nanoparticle, fluorinated polyimide, optical anisotropy, uniaxial drawing.

1. Introduction

Metal-containing polyimides were first reported by Angelo [1], who added organo-metallic complexes to several types of polyimides and reported the metallic contents, dielectric constants, and volume-resistivity for the copper-containing polyimides. Polyimide films containing metal/metal oxide particles generated *in-situ* have been studied extensively by Taylor et al. in an attempt to synthesize materials with unique electrical, magnetic, thermal, or adhesive properties.[2] They have incorporated a wide variety of metallic salts and organometallic complexes in aromatic polyimides; the number of metallic elements is more than twenty.

The present authors have synthesized and investigated the optical properties of metal (Al, Cu, Pd, Ag and Au)-containing fluorinated polyimides as novel thermally stable polymeric materials that have some interesting optical functions in the visible and the near-infrared region.[3] For investigation of the effect of the final curing temperature, polyimides were needed whose optical properties are stable over 300˚C. The fluorinated polyimides developed by the authors show almost no color and their transmittance and refractive indices are stable even after curing at 380˚C.[4] One of the polyimides is desirable for the purpose of this study as a matrix polyimide. Furthermore, distinct anisotropy in optical transmittance in the visible and near-infrared region were observed for uniaxially drawn and silver-dispersed polyimide films.[5] The films were prepared in a one-step operation that involves thermal curing and simultaneous uniaxial drawing of poly(amic acid) (PAA) films, which were made by dissolving silver nitrate in the PAA solution at a 1:4 mol ratio. The polyimide molecular chains with a rod-like structure were oriented along the drawing direction during curing, and this orientation accompanied the generation of silver nano-particles with elongated shapes. An anisotropy in optical transmittance of more than 300 (25 dB) was obtained for a 15 μm-thick film at 850 nm, and the optical loss for the transmitting polarization including surface reflection is less than 1.3 dB.[6] The optical and mechanical properties were retained after annealing at 150˚C for 1 h. Nanometer-sized metal particles are known to have inter-

Received April 2, 2002
Accepted May 23, 2002

esting optical functions such as the characteristic coloration [3] and optical non-linearity.[7] We report here the thermogravimetric analysis, x-ray diffraction patterns, transmission electron micrographs, FT-IR analysis of polymer orientations, and optical and thermal properties of uniaxially drawn and gold nanoparticle dispersed fluorinated polyimide films.

2. Experimental

2.1 *Materials*

A rod-like fluorinated polyimide, PMDA/TFDB,

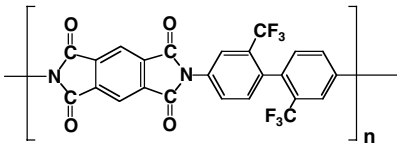

PMDA / TFDB

synthesized from pyromellitic dianhydride and 2,2'-bis(trifluoromethyl)-4,4'-diaminobiphenyl was used in this study. The preparation of poly(amic acid) (PAA), the precursor of the polyimide, and the thermal, mechanical, and optical properties of the polyimide has been described elsewhere.[4,8] Hydrogen tetrachloroaurate(III)trihydrate ($HAuCl_4 \cdot 3H_2O$) was obtained from Aldrich Chemical Co. and was used as received.

2.2 *Sample Preparation, Curing and Drawing*

Since $HAuCl_4$ showed good solubility to the *N,N*-dimethylacetamide (DMAc) solution of PAA (10 wt%, 600 poise), they were added as solids to the solutions. Addition of metallic dopant into the PAAs was in 5.7 and 13 mol%. All the synthesis and mixing procedures were performed in a nitrogen atmosphere. A globe-box was used because the source materials of PAA and the dopant are deliquescent or moisture-sensitive. The solutions were stirred for more than 12 h at room temperature and spin-coated onto a 3-inch silicon wafer.

The PAA solutions with and without dopant on substrates were dried under nitrogen at 70˚C for 1 h. For preparing uniaxially drawn Au-dispersed polyimide films, PAA films peeled from the substrate were cut into rectangular forms by 15 mm x 5 mm and loaded in a thermal mechanical analyzer (TMA: Sinku-Riko TM-7000). Constant loads were applied along the longer axis of the film by TMA during thermal curing (**Fig.1**). The film was thus heated to final curing temperature (T_f) at a heating rate of 20˚C/min, kept for each holding time, and then cooled to room temperature. The average thicknesses of the PAA and polyimide films were 22 and 15 μm, respectively.

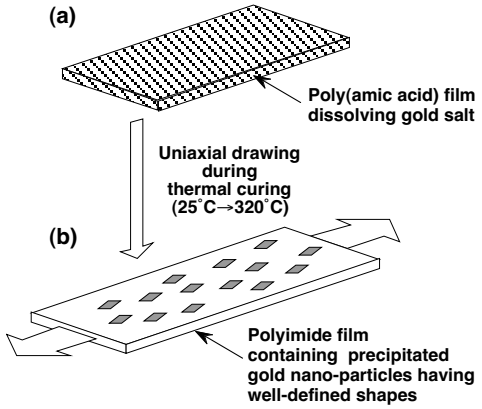

Fig. 1 Method of preparing uniaxially drawn and Au-nanoparticle-dispersed fluorinated polyimide films.

2.3 *Measurements*

2.3.1 *Wide-angle X-ray Diffraction*

Wide-angle x-ray diffraction (WAXD) patterns were obtained with a two-axis diffractometer (Phillips X'Pert MPD) for the polyimide films set on silica substrates. This diffractometer uses Cu-Ka radiation monochromatized by a silicon crystal. The x-ray beam scattered from the samples was detected by a scintillation counter through two receiving slits

2.3.2 *Transmission Electron Micrograph*

Cross-sectional transmission electron micrographs (TEM) of the gold-containing polyimides were taken with a JEOL TEM-100CX transmission electron microscope. The uniaxially drawn polyimides cured at 320˚C in air and under nitrogen were embedded in epoxy resin, and then sectioned into 60 nm thicknesses with a Reichert-Jung Werke ultra-microtome. The sectioning directions were parallel and perpendicular to the drawing direction.

2.3.3 *Polarized Vis-NIR Spectra*

The polarized transmission spectra in the visible and near-infrared region (λ = 200 to 2000 nm) were measured using a Hitachi U-3500 spectrophotometer and Advantest Q8381A optical spectrum analyzer by rotating a Glan-Thompson prism (linear polarizer) inserted into the lightpath.

2.3.4 *In-plane Birefringence Measurement*

The optical retardation of the polyimide films was measured directly by the parallel Nicole rotation method at 1.31 and 1.55 μm [9], and thickness (d) was measured from the interference fringe observed in the near-infrared absorption spectra. The retardation and the thickness were measured at the center of the films. In-plane birefringence (Δn) was calculated by dividing retardation by thickness.

2.3.5 *Polarized ATR-IR Analysis*

Attenuated total reflection (ATR)-IR spectra were measured using a Nicolet Avatar 320 FT-IR with a robust single-reflection accessory (Thunderdome,

Spectra-Tech Co. Ltd.) having a germanium IRE (45° incidence-angle) The method of estimating orientation parameter, P_{200}, for uniaxially orientated films was reported elsewhere.[10]

2.3.6 *Thermal Gravimetric Analysis*

Thermogravimetric analysis (TGA) was conducted for a small amount (about 10 mg) of undoped and Au-doped PAA films peeled from the substrates using a Shimadzu TGA-50 analyzer. PAA films were heated to 900˚C at 10˚C/min under nitrogen.

3. Results and Discussion

Fig.2 shows the WAXD patterns of uniaxially drawn Au-dispersed polyimide films cured under nitrogen and in air. Distinct diffraction peaks are observed, and all of these are assigned to crystalline gold. This indicates that the dopant ($HAuCl_4 \cdot 3H_2O$) was reduced to zero-valent state and crystallized in the polyimide films. Note that no peaks are observed for [200], [311], [331], and [422], which are usually observed for polycrystalline gold (see the reference data). This indicates that the [111], [220], and [222] lattices of Au are preferentially formed along the film surface during curing. A similar phenomenon was observed for unoriented Au-dispersed film.[3] In addition, broad diffraction peaks (not shown) are observed at 16.1˚ and 24.2˚, which are assigned to the lateral order of uniaxially oriented polyimide chains and amorphous halo, respectively.[11]

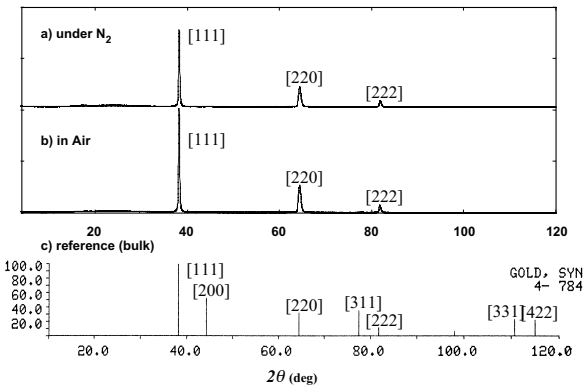

Fig. 2 X-ray diffraction patterns of Au-nanoparticle dispersed polyimide films prepared (a) under N_2 and (b) in air and (c) refrenece data of gold polycrystallites.

Figs.3 and 4 show the cross sectional TEM micrographs of a film prepared under nitrogen. An

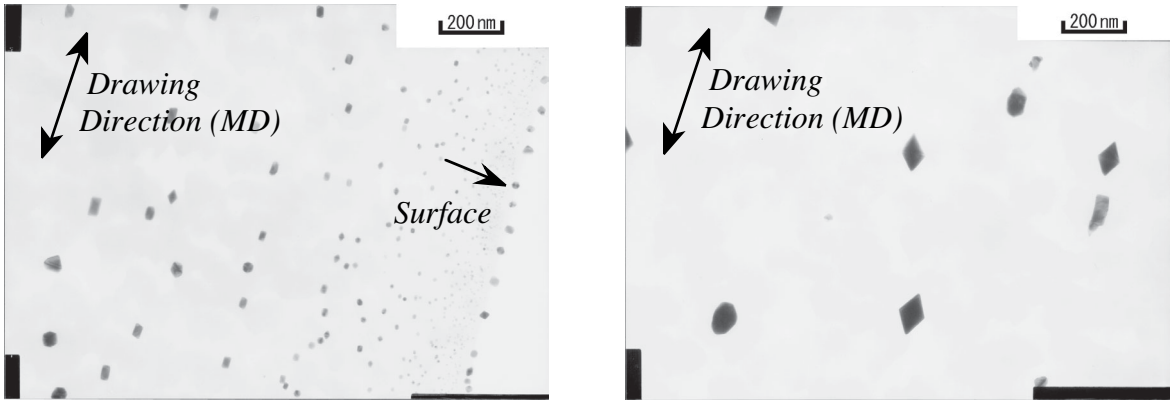

Fig. 3 Cross sectional TEM micrograph (x 50,000) of Au-nanoparticle dispersed polyimide film prepared under N_2. The sectioning direction was parallel to the drawing direction. Micrograph of a part close to the surface (Left) and a part in the midst of film (Right). The long axes of the precipitated Au-particles inside the film are oriented along the drawing direction.

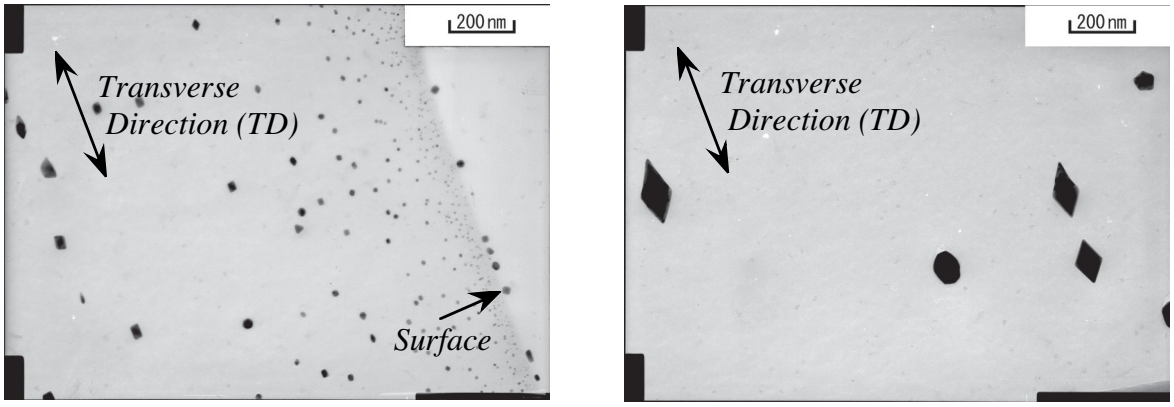

Fig. 4 Cross sectional TEM micrograph (x 50,000) of Au-nanoparticle dispersed polyimide film prepared under N_2. The sectioning direction was perpendicular to the drawing direction. Micrographs of a part close to the surface (Left) and a part in the midst of film (Right). The long axes of the precipitated Au-particles inside the film are oriented along the tranverse direction.

Au-dispersed film was sectioned along the two directions; parallel (*MD*, Fig.3) and perpendicular (*TD*, Fig.4) to the drawing direction. The Au-particles precipitated are distributed uniformly through the film, but the sizes of the particles varied in a very wide range from the surface to the midst of film. Very small particles (less than 10 nm) are precipitated near the surface (left-hand side), though relatively large particles are observed on the surface. And the sizes of particles gradually increase as the distance from the surface increases. In contrast, the sizes of Au crystallites in the midst of film (right-hand side, 100-150 nm) are much larger than those near the surface. A striking feature of the particles is their anisotropic and well-defined lozenge (diamond) or rectangular shapes. A typical size of lozenge particles is 130 x 100 nm. In addition, most of them are oriented in the direction parallel to the surface (film plane). They are also oriented along the drawing direction (*MD*) in Fig.3 and are oriented perpendicular to the drawing direction (*TD*). This should be related to the preferential ordering of the [111] lattice along the film surface. The similarity of the particle shapes in Figs. 3 and 4 indicates that most of the particles have pressed octahedron and rectangular parallelepiped structures of the crystallites. In an Au-dispersed film formed on SiO_2 substrate, particles having rectangular shapes were observed [3], but no lozenge-shaped particles were observed. Micrographs of a film prepared in air are basically the same as Figs. 3 and 4, while the average size of Au-particles precipitated in air is slightly larger.

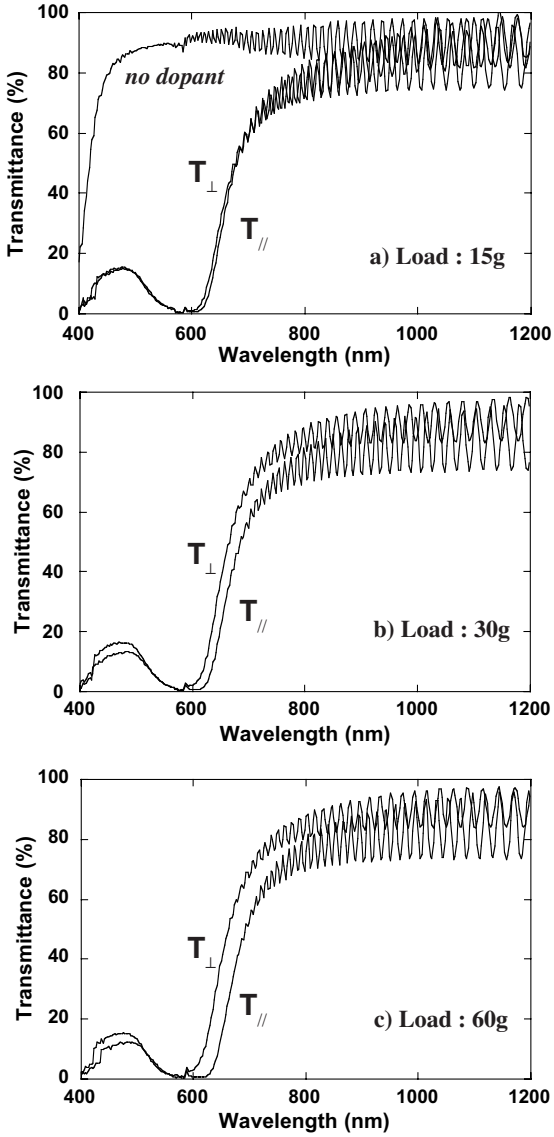

Fig. 5 Optical absorption spectra of Au-nanoparticle dispersed polyimide films uniaxially drawn with constant loads under N_2 at T_f=345°C for 120 min.

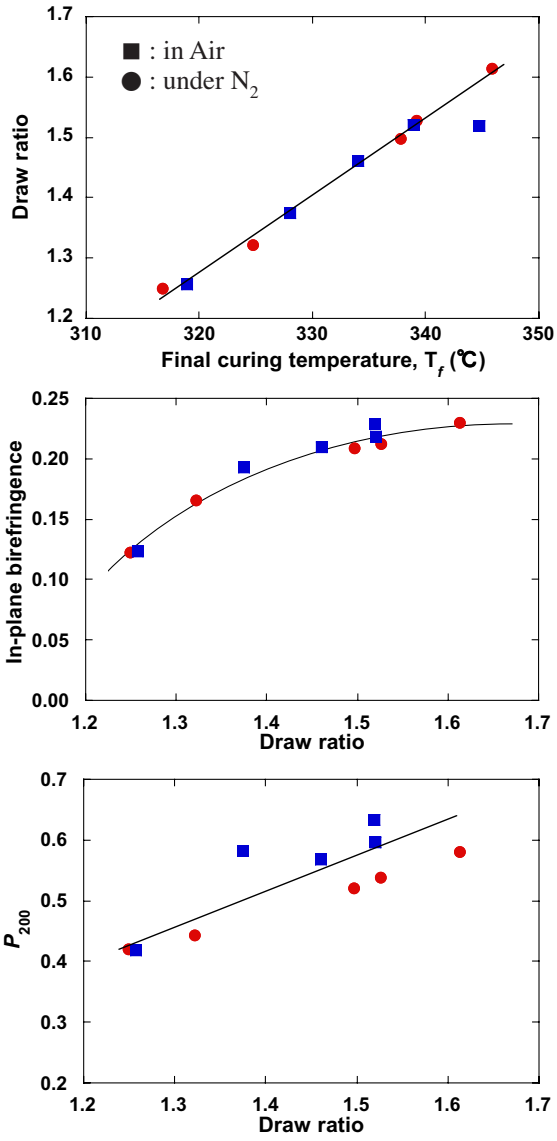

Fig. 6 Relationships between T_f, draw ratio, in-plane birefringence (Δn), and orientation parameter P_{200} for Au-dispersed polyimide films prepared at different T_f with a constant load of 60 g. (holding time :120 min.)

Fig.5 shows the polarized optical transmission spectra of Au-nanoparticle dispersed polyimide films uniaxially drawn with constant loads. In contrast to the very pale yellow color of undoped film, the dark purple color of Au-dispersed films originates from the surface plasmon absorption of nanometer-sized gold particles. This is well characterized by the strong absorptions around 600 nm. In addition, small but distinct anisotropy in optical transmission is observed for the films that were uniaxially drawn with large loads. This suggests that the Au-particles having anisotropic shapes are preferentially oriented along the drawing direction. In addition, the optical anisotropy should be related to the degree of orientation of polyimide chains.

Fig. 6 shows the relationships between T_f, draw ratio, in-plane birefringence (Δn), and orientation parameter P_{200}. Although draw ratio is linearly proportional to T_f, Δn does not increase in the same manner at larger draw ratios. Δn is a good measure of in-plane orientation of polyimide chains, and no difference was observed between the films uniaxially drawn under N_2 and in air. On the other hand, P_{200} is nearly proportional to the draw ratio, and note that the values of P_{200} for the films prepared in air are larger than those under N_2. This indicates that the total degree of orientation in the former is larger than the latter, which is well reflected on the larger dichroic ratios (D) at 670 nm of the former than the latter (**Fig.7**). The value of D increases as the draw ratio increases, but the dependence is not significant.

Figs. 8 and 9 show polarized optical absorption spectra of Au-dispersed polyimide films uniaxially drawn under different atmosphere. The surface plasmon absorption peak parallel to the drawing direction ($A_{//}$) is displaced to a longer wavelength than that perpendicular to the drawing direction ($A_{\perp}$). This is the main cause of the optical anisotropy (*i.e.* dichroic ratio) observed at a certain range of wavelengths

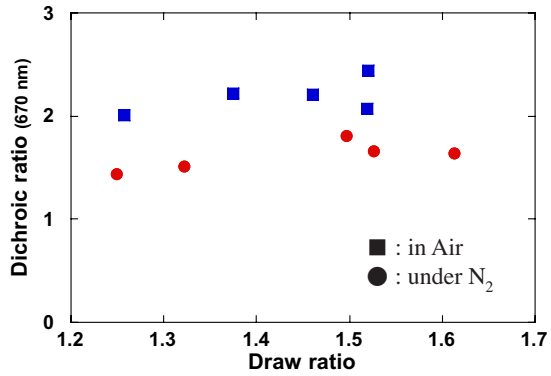

Fig. 7 Relationship between the draw ratio and dichroic ratio at 670 nm for Au-dispersed polyimide films prepared at different T_f with a constant load (60 g) and a holding time (120 min). (● : under N_2, ■ : in Air)

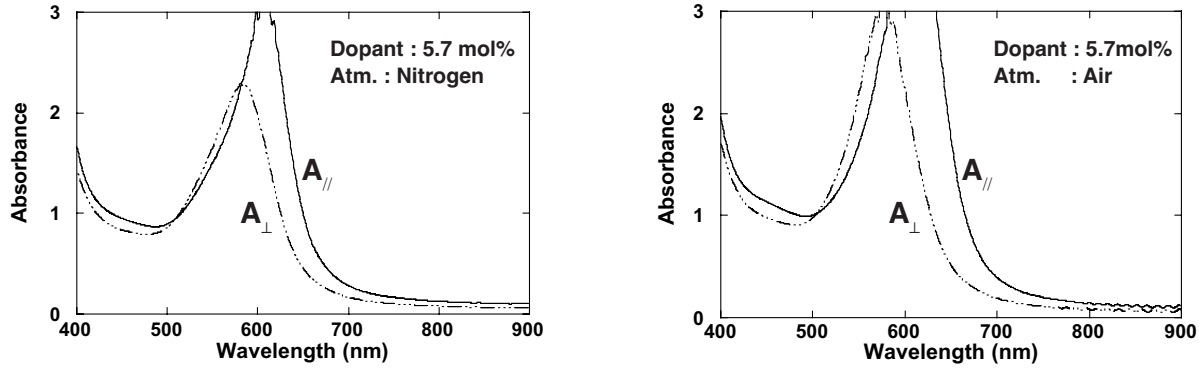

Fig. 8 Absorption spectra of Au-dispersed polyimide films uniaxiallly drawn under different atmosphere with a constant load (60 g) at T_f=345°C for 120 min. (a) Under N_2 and (b) in air. The content of Au-dopant was 5.7 mol%.

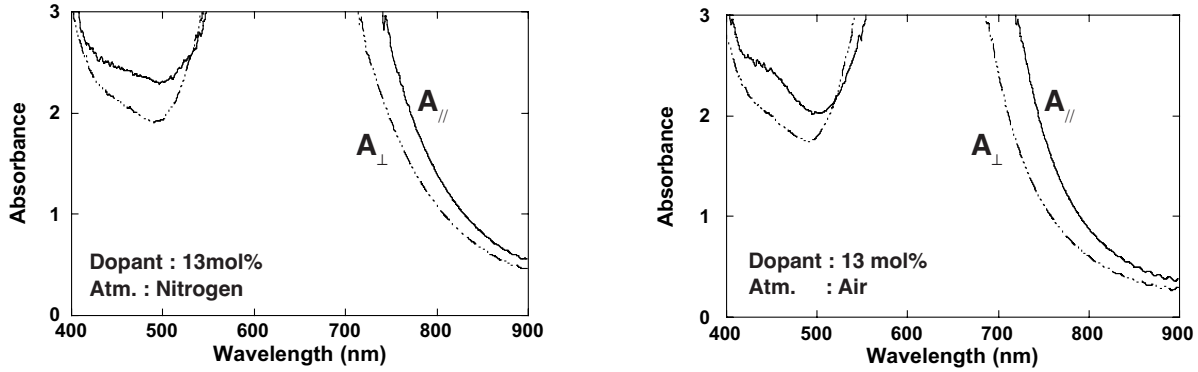

Fig. 9 Absorption spectra of Au-dispersed polyimide films uniaxiallly drawn under different atmosphere with a constant load (60 g) at T_f=345°C for 120 min. (a) Under N_2 and (b) in air. The content of Au-dopant was 13 mol%.

Table 1 Center wavelengths (λ, nm) and anisotropies in λ (Δλ) of plasmon absorptions for Au-dispersed polyimids uniaxiallly drawn under different atmosphere. The spectra are shown in Figs. 8 and 9.

Conc.	under N_2			in Air		
	$\lambda_\perp$	$\lambda_{//}$	$\Delta\lambda$	$\lambda_\perp$	$\lambda_{//}$	$\Delta\lambda$
5.7 mol%	590	610	20	575	605	30
13.0 mol%	625	645	20	620	645	25

(600-700 nm). When the concentration of dopant is increased from 5.7 to 13 mol%, the plasmon absorption becomes much stronger, and its center wavelength and absorption edge are displaced to longer wavelengths as listed in Table 1.

This indicates that the average size of Au-particles increases under a high dopant concentration, and thus the optical anisotropy is observed at longer wavelengths (700-800 nm). In addition, the peak displacements between 5.7 and 13.0 mol% are 35 nm for the film prepared under N_2, while those for the film prepared in air are 40-45 nm. This also supports the larger optical anisotropy of the latter. Furthermore, the uniaxially drawn Au-dispersed polyimide films exhibit high transparency in the near-infrared (NIR) region (λ=800-2000 nm). In contrast, the transparency of Au-dispersed polyimide films cured on SiO_2 substrates was less than 10% in the NIR region, which is due to the significant growth of Au-crystallites on the substrate-side surface.[3] This indicates that the films prepared in this study can be used as thin and flexible visible-cut/NIR-pass optical filters.

Fig.10 shows TGA curves of undoped and Au-doped PAA films. The weight loss below 250˚C was caused by imidization reaction (evaporation of water). The curves of Au-dispersed polyimides are basically same as that of undoped polyimide, although slight acceleration of weight decrease is observed above 400˚C. This indicates that precipitated Au-nanoparticles does not cause substantial degradation of polyimide structure. Fluorinated poly imide is a good host-material for Au-nanoparticles.

4. Conclusions

Gold-nanoparticle dispersed fluorinated polyimide films were prepared by thermal curing and uniaxially drawing of poly(amic acid) films containing $HAuCl_4 \cdot 3H_2O$ as a dopant. The gold salt was converted into zero-valent gold (Au) particles having high crystallinity after thermal imidization. The preferential ordering of [111] lattice along the film surface was observed. Precipitated Au-particles are distributed uniformly through the film, but the sizes

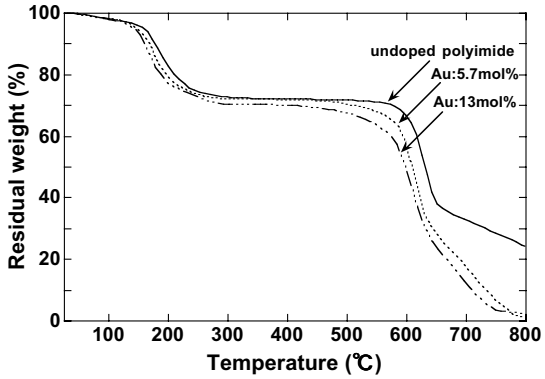

Fig. 10 TGA curves of (a) undoped and Au-doped polyimide films with (b) 5.7 mol% and (c) 13mol%.

of the particles varied in a very wide range from the surface to the midst of film. They exhibit well-defined lozenge or rectangular shapes, which suggest pressed octahedron or rectangular parallelepiped structures of the crystallites. The long axis of the crystallites are oriented along the surface direction and along the directions parallel or perpendicular to the drawing direction. The films show high absorption in the visible region than the host-polyimide, which is due to the surface plasmon absorption of Au-nanoparticles. In addition, significant anisotropy in optical transmittance were observed for the doped films uniaxially drawn with large loads, which indicates anisotropic shapes of Au-particles. The films prepared in air showed larger optical anisotropy than those prepared under N_2. This agrees well with the fact that the orientation parameter P_{200} of polyimide chains in the former films is slightly larger than the latter.

References

1. R. J. Angelo, U.S.Patent 3,073,785 (1959).
2. M.W. Ellison and L.T. Taylor, *Chem. Mater.*, **6**, (1994) 990 and the references therein.
3. T. Sawada and S. Ando, *Chem. Mater.*, **10** (1998) 3368.
4. T. Matsuura, S. Ando, S. Sasaki, and F. Yamamoto, *Macromolecules*, **27** (1994) 6665.
5. T. Sawada, S. Ando, and S. Sasaki, *Appl. Phys. Lett.*, **74** (1999) 938.
6. S. Matsuda, S. Ando, and T. Sawada, *Electron. Lett.*, **37** (2001) 706.
7. *Non-linear Optics of Organics and Semiconductors*; Kobayashi, T. Ed.; Springer-Verlag: Berlin, 1989; Part II.
8. T. Matsuura, Y. Hasuda, S. Nishi, Y. Yamada, *Macromolecules*, **24** (1991) 5001.
9. S. Ando, T. Sawada, and S. Sasaki, *Polym. Adv. Technol.*, **12** (2001) 319.
10. S. Matsuda and S. Ando (*submitted for publication*).
11. S.M. Pyo, S.I. Kim, T.J. Shin, Y.H. Park, and M. Lee, *J. Polym. Sci., Part A. Polym. Chem.*, **37** (1999) 937.